

Distances and lensing in cosmological void models

Kenji Tomita

Yukawa Institute for Theoretical Physics, Kyoto University, Kyoto 606-8502, Japan

tomita@yukawa.kyoto-u.ac.jp

ABSTRACT

We study the distances and gravitational lensing in spherically symmetric inhomogeneous cosmological models consisting of inner and outer homogeneous regions which are connected by a single shell or double shells at the redshift $z_1 \sim 0.067$. The density and Hubble parameters in the inner region are assumed to be smaller and larger, respectively, than those in the outer region. It is found that at the stage $z_1 < z < 1.5$ the distances from an observer in the inner void-like region are larger than the counterparts (with equal z) in the corresponding homogeneous Friedmann models, and hence the magnitudes for the sources at this stage are larger. This effect of the void-like low-density region may explain the deviations of the observed [magnitude-redshift] relation of SNIa from the relation in homogeneous models, independently of the cosmological constant. When the position of the observer deviates from the center, moreover, it is shown that the distances are anisotropic and the images of remote sources are systematically deformed. The above relation at $z \gtrsim 1.0$ and this anisotropy will observationally distinguish the role of the above void-like region from that of the positive cosmological constant. The influence on the time-delay measurement is also discussed.

Subject headings: cosmology: large scale structure of the universe - observations

1. Introduction

In recent cosmological observations, the following three remarkable phenomena have been discovered, which may contradict with the homogeneity of the universe. One of them is the large-scale bulk flows in the region with distance $< 150h^{-1}$ Mpc ($H_0 = 100h^{-1}$ km sec $^{-1}$ Mpc $^{-1}$) without the associated large CMB dipole anisotropy (Hudson et al. 1999; Willick 1999). Second we have the inhomogeneity of the observed Hubble constant whose values are smaller in the measurements for remoter sources (Branch 1998; Freedman 1997; Sandage and Tammann 1997; Blandford and Kundić 1997). The last one is the magnitude-redshift relation of SNIa, in which the observed magnitudes of sources are larger than those expected in the homogeneous Friedmann models without the cosmological constant. For the model-fitting the positive cosmological constant which brings an “accelerating” universe was considered as a necessary quantity (Riess et al. 1998; Schmidt et al. 1998; Garnavich et al. 1998).

For the explanation of the first phenomenon we considered spherically symmetric inhomogeneous models in a previous paper (Tomita 1999), which is cited as paper I in the following. They consist of inner and outer homogeneous regions connected with a single shell, double shells or an intermediate self-similar region (Tomita 1996, 1995), and it is assumed that the density and Hubble parameters in the inner region are smaller and larger, respectively, than those in the outer region. Then it was shown that the observed situation of bulk flows and CMB dipole anisotropy can be reproduced, if the radius of the boundary of the two region and the observer’s position from the center are about $200h^{-1}$ Mpc and $40h^{-1}$ Mpc, respectively. The consistency with the observed bulk flows (Hudson et al. 1999; Willick 1999; Dale et al. 1999; Giovanelli et al. 1998) was shown in paper I. These models are found to be consistent also with the observed inhomogeneity of the Hubble constant.

The inhomogeneity of the Hubble constant has already been discussed by various workers (e.g. Turner et al. (1992), Bartlett et al. (1995)). The local void region with higher Hubble constant was studied independently by Zehavi et al. (1998) as the local Hubble bubble, which has the scale $\sim 70h^{-1}$ Mpc and is bordered by the dense walls as the Great Attractor. They analyzed the statistical relation between the distances and the local Hubble constants derived from the data of SNIa, and found the existence of a void region with a local Hubble constant larger than the global Hubble constant. The relation to the SNIa data on the scale $\sim 150h^{-1}$ Mpc will be discussed in this paper from our standpoint.

In the present paper the behavior of the distances is investigated in the models in the previous paper with similar model parameters. In §2, we treat the distances from a virtual observer who is in the center of the inner void-like region in models with a single shell, and derive the [magnitude m - redshift z] relation. This relation is compared with the counterpart in the homogeneous models. Then the relation in the present models is found to deviate from that in the homogeneous models with $\Lambda = 0$ at the stage of $z < 1.5$. It is partially similar to that in the nonzero- Λ homogeneous models, but the remarkable difference appears at the high-redshift stage $z > 1.0$. In §3, we consider a realistic observer who is in the position deviated from the center, and calculate the distances from him. The distances depend on the direction of incident light and the area angular diameter distance is different from the linear angular diameter distances. It is shown as the result that the $[m, z]$ relation is anisotropic, but the relation averaged with respect to the angle is very near to the relation by the virtual observer. The comparison with the observed relation for SNIa is also discussed. In §4 we derive the lens effect such as the convergence and shear of the images caused by the above anisotropic nature of distances, and in §5 discuss the influence on the time-delay from a remote double quasar. §6 is dedicated to concluding remarks. In Appendix A, the derivation of distances in models with double shells is described in parallel with §2 and §3.

2. Distances from the center of the inner region

In this section we treat the models with a single shell, in which the inner homogeneous region V^I and the outer homogeneous region V^{II} are connected with a shell and the lineelement is expressed as

$$ds^2 = g_{\mu\nu}^j(dx^j)^\mu(dx^j)^\nu = -c^2(dt^j)^2 + [a^j(t^j)]^2 \left\{ d(\chi^j)^2 + [f^j(\chi^j)]^2 d\Omega^2 \right\}, \quad (1)$$

where j ($= I$ or II) represents the regions, $f^j(\chi^j) = \sin \chi^j, \chi^j$ and $\sinh \chi^j$ for $k^j = 1, 0, -1$, respectively, and $d\Omega^2 = d\theta^2 + \sin^2 \theta \varphi^2$. The model parameters are expressed as H_0^j ($= 100h_0^j$), Ω_0^j and λ_0^j . Here the negative curvature is assumed in all regions. In the paper I, we showed the Einstein equations in both regions and the junction conditions at the boundary shell which is given as $\chi^I = \chi_1^I$ and $\chi^{II} = \chi_1^{II}$, and derived the equations of light rays in both regions.

Using the latter equations we obtained CMB dipole and quadrupole anisotropies and found that the influence of motions of the shell on the light paths is negligibly small, so that the approximation of the comoving shell is good for the treatment of light rays. In this paper this approximation is assumed throughout in all cases, and the equations in the paper I are cited as Eq. (I.2.1), Eq.(I.A1) and so on.

The angular diameter distance d_A between a virtual observer at the center O (in the inner region V^I) and the sources S is given by

$$d_A = a^I(\bar{\eta}_s^I) \sinh(\bar{\chi}_s^I), \quad (2)$$

if S is in V^I , where $(\bar{\eta}_s^I, \bar{\chi}_s^I)$ are the coordinates of S. Here and in the following, bars are used for the coordinates along the light paths to the virtual observer, as in the paper I. If S is in V^{II} , we have

$$d_A = a^I(\bar{\eta}_1^I) \sinh(\bar{\chi}_1^I) + [a^{II}(\bar{\eta}_s^{II}) \sinh(\bar{\chi}_s^{II}) - a^{II}(\bar{\eta}_1^{II}) \sinh(\bar{\chi}_1^{II})] = a^{II}(\bar{\eta}_s^{II}) \sinh(\bar{\chi}_s^{II}), \quad (3)$$

where Eq. (I.2.2) for R was used. When S is in V^I , $(\bar{\eta}_s^I, \bar{\chi}_s^I)$ are related to $(\bar{\eta}_0^I, 0)$ by

$$\bar{\eta}_0^I - \bar{\eta}_s^I = \bar{\chi}_s^I, \quad (4)$$

where $\bar{\eta}_0^I$ is given by Eqs. (I.2.13) and (I.2.14) with $y^I = 1$, and $\bar{\eta}_s^I$ is related to the source redshift \bar{z}_s^I by

$$1 + \bar{z}_s^I = 1/(\cosh \bar{\eta}_s^I - 1). \quad (5)$$

For a given \bar{z}_s^I , we obtain $\bar{\eta}_s^I$ and $\bar{\chi}_s^I$, and hence d_A from Eq. (2).

When S is in V^{II} , we have

$$\bar{\eta}_0^I - \bar{\eta}_1^I = \bar{\chi}_1^I \quad (6)$$

and

$$\bar{\eta}_1^{II} - \bar{\eta}_s^{II} = \bar{\chi}_s^{II} - \bar{\chi}_1^{II}, \quad (7)$$

where $\bar{\eta}_1^I$ is related to \bar{z}_1^I by

$$1 + \bar{z}_1^I = 1/(\cosh \bar{\eta}_1^I - 1) \quad (8)$$

and so $\bar{\chi}_1^I$ is also related to \bar{z}_1^I using Eq. (6). Coordinates at the shell, $(\bar{\eta}_1^I, \bar{\chi}_1^I)$ and $(\bar{\eta}_1^{II}, \bar{\chi}_1^{II})$ are connected by Eqs. (I.3.23) and (I.3.24). On the other hand, $\bar{\eta}_s^{II}$ is related to \bar{z}_s^{II} by

$$\frac{1 + \bar{z}_s^{II}}{1 + \bar{z}_1^{II}} = \frac{\cosh \bar{\eta}_1^{II} - 1}{\cosh \bar{\eta}_s^{II} - 1}, \quad (9)$$

where \bar{z}_1^{II} is equal to \bar{z}_1^I under the approximation of the comoving shell (cf. Eq. (I.2.6)). Accordingly, d_A is uniquely determined for given \bar{z}_1^I ($= \bar{z}_1^{II}$) and \bar{z}_s^{II} .

The distance (d_A^F) in a homogeneous Friedmann model is

$$d_A^F = a^I(\bar{\eta}_s^I) \sinh \bar{\chi}_s^I, \quad (10)$$

which is defined in V^I for arbitrary \bar{z}_1^I , assuming that V^I covers every region of the model.

The luminosity distances d_L and d_L^F are defined in terms of $d_A d_A^F$ as $d_L = (1+z)^2 d_A$ and $d_L^F = (1+z)^2 d_A^F$. Accordingly the ratio of luminosity distances is equal to the ratio of angular diameter distances. In Figs. 2 and 3 the behavior of $5 \log d_L$ as a function of z ($= \bar{z}_s^j$) is shown in the case of $\bar{z}_1^I = 0.067$ for the parameters $(\Omega_0^I, \Omega_0^{II}, h^I, h^{II}/h^I) = (0.2, 0.56, 0.7, 0.82)$ and $(0.2, 0.88, 0.7, 0.82)$, respectively, which are appropriate to describe the bulk flow in the previous paper (Tomita 1999). The lines in the homogeneous models with $(\Omega_0, \lambda_0) = (0.2, 0)$ and $(0.2, 0.8)$ are also shown for comparison. It is found that $5 \log d_L$ is larger than that in the model with $(0.2, 0)$ for $\bar{z}_1^I < z < 1.5$, it is consistent with that in the model with $(0.2, 0.8)$ for $0.1 < z < 0.3$, and it is intermediate for $0.1 < z < 1.0$ between the two models with $(0.2, 0)$ and $(0.2, 0.8)$. The difference between the present shell model and the non-zero λ_0 model is remarkable for $z > 1.0$. According to recent data of high-redshift SNIa (Riess et al. 1998; Schmidt et al. 1998; Garnavich et al. 1998), it is at epochs of $z \sim 0.4$ that their data of m deviate conspicuously from the values in the homogeneous models with vanishing cosmological constant. From the comparison with their data, it seems that the present models can explain their data as well as the non-zero λ_0 model.

In Fig. 4 the behavior of $5 \log d_L$ (by the observer at C) in the double-shell models is shown for $\bar{z}_1^I = 0.05$ and $\bar{z}_2^{II} = 0.1$, where the distances in the double-shell case are derived in the Appendix A. It is found that the general trend is same as that in the single-shell case.

In Figs. 5 and 6, the magnitude differences Δm [$\equiv 5 \log d_L - 5 \log(d_L)_{\text{homog}}$] are shown in the single-shell and double-shell cases, respectively. In Fig. 5 the difference for $\Omega_0 = 0.3$ is also shown and it is found to be smaller than that for $\Omega_0 = 0.2$.

3. Distances from a non-central observer O in the inner region

Next let us derive the angular diameter distance d_A from an observer O whose position is deviated from the center. When the source S is in V^I , d_A is equal to d_A^F in the homogeneous Friedmann model. In the following we consider the case when S is in the outer regions. In this

case we have two linear angular diameter distances (the longitudinal linear distance d_A^l and the transverse linear distance d_A^t) for the angles in the φ and θ directions, respectively, and the area angular diameter distance d_A^a [$\equiv (d_A^l d_A^t)^{1/2}$] (cf. Fig. 7).

Let us consider a single-shell model and assume that, in the plane $\theta = \text{const}$, two light rays start from S at $(\eta_s^{\text{II}}, \chi_s^{\text{II}}, \varphi_s)$ and $(\eta_s^{\text{II}}, \chi_s^{\text{II}}, \varphi_s + \Delta\varphi_s)$ and reach O at $(\eta_0^{\text{I}}, \chi_0^{\text{I}}, 0)$ with the angle ϕ and $\phi + \Delta\phi$, respectively. If the angular diameter distance from S to the center C is $d_A(\eta_s^{\text{II}}, \chi_s^{\text{II}})$, the proper interval of the two rays in S is equal to $d_A(\eta_s^{\text{II}}, \chi_s^{\text{II}})d\varphi_s$, so that the longitudinal linear distance is defined by

$$d_A^l \equiv d_A(\eta_s^{\text{II}}, \chi_s^{\text{II}}) \partial\varphi_s / \partial\phi / [\cos(\phi - \varphi_s)], \quad (11)$$

where $d_A(\eta_s^{\text{II}}, \chi_s^{\text{II}})$ is given by

$$d_A(\eta_s^{\text{II}}, \chi_s^{\text{II}}) = a^{\text{II}}(\eta_s^{\text{II}}) \sinh(\chi_s^{\text{II}}). \quad (12)$$

Next let us consider two rays with equal ϕ in planes of $\theta = 0$ and $\Delta\theta$, when $\Delta\theta \ll \pi$. Then [the angle between two rays reaching O] ($= \Delta\theta \sin \varphi_s$) is equal to [the angle between two rays reaching C] multiplied by a factor ($\sin \phi / \sin \varphi_s$). Therefore the transverse linear distance is

$$d_A^t = d_A(\eta_s^{\text{II}}, \chi_s^{\text{II}}) \sin \varphi_s / \sin \phi. \quad (13)$$

In the following we derive the relations between $(\eta_s^{\text{II}}, \chi_s^{\text{II}}, \varphi_s)$, $(\eta_0^{\text{I}}, \chi_0^{\text{I}}, 0)$ and the incident angle ϕ . When we give the redshift z_1^{I} , the radial coordinate χ_1^{I} is fixed using Eqs. (6) and (8).

In V^{I} we have Eq. (I.3.10) for η_1^{I} in the case of $\phi = \phi_1$ and $\pi - \phi_1$, and

$$h_0^{\text{I}} = [1 + (\zeta^{\text{I}})^2]^{1/2}, \quad \zeta^{\text{I}} = \sinh \chi_0^{\text{I}} \sin \phi, \quad (14)$$

where χ_0^{I} is fixed by giving the distance CD, that is,

$$l_0 = a_0 \chi_0^{\text{I}}. \quad (15)$$

For $(\eta_s^{\text{II}}, \chi_s^{\text{II}})$ we obtain from Eq. (I.3.11)

$$G(\chi_s^{\text{II}}) \equiv \cosh^{-1} \left(\frac{\cosh \chi_s^{\text{II}}}{h_0^{\text{II}}} \right) - \cosh^{-1} \left(\frac{\cosh \chi_1^{\text{I}}}{h_0^{\text{II}}} \right) = \eta_1^{\text{II}} - \eta_s^{\text{II}}. \quad (16)$$

The definition (I.3.7) of h_0^j and the junction conditions (I.3.16) and (I.3.17) lead to

$$h_0^{\text{II}} = [1 + (\zeta^{\text{II}})^2]^{1/2}, \quad \zeta^{\text{II}} = \frac{a_0^{\text{I}}}{a_0^{\text{II}}} \zeta^{\text{I}}, \quad (17)$$

where A_0^j ($j = \text{I}, \text{II}$) are given by Eq. (I.2.12). The coordinates at the boundary $(\eta_1^{\text{II}}, \chi_1^{\text{II}})$ in Eq. (16) are related to $(\eta_1^{\text{I}}, \chi_1^{\text{I}})$, using

$$a_0^{\text{I}} y^{\text{I}}(\eta_1^{\text{I}}) \sinh \chi_1^{\text{I}} = a_0^{\text{II}} y^{\text{II}}(\eta_1^{\text{II}}) \sinh \chi_1^{\text{II}} \quad (18)$$

and

$$a_0^I \int_0^{\eta_1^I} y^I(\eta) d\eta = a_0^{II} \int_0^{\eta_1^{II}} y^{II}(\eta) d\eta, \quad (19)$$

which are derived from Eq. (I.2.2) for R and Eq. (I.2.6) with $\gamma^I = \gamma^{II} = 1$. Therefore, η_s^{II}, χ_s^{II} are determined by specifying the values of $\bar{z}_1^I, \bar{z}_s^{II}$ and ϕ_1 .

Next let us derive φ by integrating the ray equations

$$\frac{d\varphi}{d\chi^j} = \frac{(k\varphi)^j}{(k\chi)^j}, \quad (20)$$

where $(k\varphi)^j$ and $(k\chi)^j$ for $j = I$ and II are shown in Eqs. (I.3.2) and (I.3.3). The solution of (20) satisfying the conditions that $\varphi(\chi = \chi_0) = 0$ and $\varphi(\chi > 0) \rightarrow \phi$ for $\chi_0 \rightarrow 0$ is

$$\begin{aligned} \varphi = & \tan^{-1} \left\{ \frac{1}{\zeta^I} \left[\sinh^2 \chi^I + \cosh \chi^I \sqrt{\sinh^2 \chi^I - (\zeta^I)^2} \right] \right\} \\ & - \tan^{-1} \left\{ \frac{1}{\zeta^I} \left[\sinh^2 \chi_0^I + \cosh \chi_0^I \sqrt{\sinh^2 \chi_0^I - (\zeta^I)^2} \right] \right\} \end{aligned} \quad (21)$$

and

$$\begin{aligned} \varphi = & \tan^{-1} \left\{ \frac{1}{\zeta^I} \left[\sinh^2 \chi^I - \cosh \chi^I \sqrt{\sinh^2 \chi^I - (\zeta^I)^2} \right] \right\} \\ & - \tan^{-1} \left\{ \frac{1}{\zeta^I} \left[\sinh^2 \chi_0^I - \cosh \chi_0^I \sqrt{\sinh^2 \chi_0^I - (\zeta^I)^2} \right] \right\}. \end{aligned} \quad (22)$$

Solutions (21) and (22) are applicable for $k^j > 0$ and < 0 , respectively.

In V^I we have for $\phi = \phi_1$

$$\varphi = \tan^{-1} \left\{ \frac{1}{\zeta^I} \left[\sinh^2 \chi^I + \cosh \chi^I \sqrt{\sinh^2 \chi^I - (\zeta^I)^2} \right] \right\}, \quad (23)$$

$$\varphi_1 = \varphi(\chi^I = \chi_1^I). \quad (24)$$

For $\phi = \pi - \phi_1$

$$\begin{aligned} \varphi = & \tan^{-1} \left\{ \frac{1}{\zeta^I} \left[\sinh^2 \chi^I - \cosh \chi^I \sqrt{\sinh^2 \chi^I - (\zeta^I)^2} \right] \right\} \\ & - \tan^{-1} \left\{ \frac{1}{\zeta^I} \left[\sinh^2 \chi_0^I - \cosh \chi_0^I \sqrt{\sinh^2 \chi_0^I - (\zeta^I)^2} \right] \right\}, \end{aligned} \quad (25)$$

$$\varphi_m = \varphi(\chi^I = h i_m^I) \quad (26)$$

in the interval $\chi_0 < \chi \leq \chi_m$, and

$$\begin{aligned} \varphi = \varphi_m & + \tan^{-1} \left\{ \frac{1}{\zeta^I} \left[\sinh^2 \chi^I + \cosh \chi^I \sqrt{\sinh^2 \chi^I - (\zeta^I)^2} \right] \right\} \\ & - \tan^{-1} \left\{ \frac{1}{\zeta^I} \left[\sinh^2 \chi_m^I + \cosh \chi_m^I \sqrt{\sinh^2 \chi_m^I - (\zeta^I)^2} \right] \right\}, \end{aligned} \quad (27)$$

$$\varphi_1 = \varphi(\chi^I = \chi_1^I) \quad (28)$$

in the interval $\chi_m < \chi \leq \chi_1$.

In V^{II} we have

$$\begin{aligned} \varphi = \varphi_1 &+ \tan^{-1} \left\{ \frac{1}{\zeta^{II}} \left[\sinh^2 \chi^{II} + \cosh \chi^{II} \sqrt{\sinh^2 \chi^{II} - (\zeta^{II})^2} \right] \right\} \\ &- \tan^{-1} \left\{ \frac{1}{\zeta^{II}} \left[\sinh^2 \chi_1^{II} + \cosh \chi_1^{II} \sqrt{\sinh^2 \chi_1^{II} - (\zeta^{II})^2} \right] \right\}, \end{aligned} \quad (29)$$

$$\varphi_s = \varphi(\chi^{II} = \chi_s^{II}). \quad (30)$$

Thus φ_s was derived as a function of \bar{z}_1^I , z_s^{II} and ϕ ($= \phi_1$ or $\pi - \phi_1$). d_A^l , d_A^t and d_A^a depend on the angle ϕ . Here we calculate the average value of d_A^a defined by

$$\langle d_A^a \rangle = \frac{1}{2} \int_0^\pi d_A^a \sin \phi d\phi. \quad (31)$$

The z dependence of average values of the corresponding luminosity distance d_L^a ($= (1+z)^2 d_A^a$) are shown in Figs. 2 and 3 in comparison with the distance by the observer C. It is found that, in almost all range of z , two lines indicating these two distances are overlapped and cannot be distinguished. As for the average behavior of distances from the observer O, therefore, we can approximately use the distances from the observer C for the former ones.

4. Lensing due to the inhomogeneity

When the observer's position (O) deviates from the center (C) of the inner region, the area distance from the observer is anisotropic and the two linear distances are not equal. This is a lens effect caused by the anisotropic and inhomogeneous matter distribution around the observer (O). Here we discuss the ϕ dependence of the area distance and the ratio of the two linear distances d_A^l/d_A^t .

4.1. Area angular diameter distance

The angular diameter distance is largest and smallest in the directions of $\phi = 0$ and π , respectively. This is because light in the directions of $\phi = 0$ and π spends the longest and shortest time in V^{II} , respectively. The behavior of m is also similar. Here we consider m for the distance and treat the magnitude difference Δm ($\equiv m - m_{\text{homog}}$), where m_{homog} is the magnitude in the Friedmann model with the same Ω_0 . The z dependence of the magnitude difference Δm for the observer O was derived in the single-shell models. In Figs. 8 and 9, the values averaged for $\phi < \pi/4$, $\pi/4 < \phi < 3\pi/4$, and $\phi > 3\pi/4$ are shown. The difference between $\Delta m(\phi < \pi/4)$ and $\Delta m(\phi > 3\pi/4)$ reaches ~ 0.4 mag at the epoch $z \sim 0.1$. This difference may represent large dispersions in m around this epoch. To confirm observationally whether there exists this anisotropy in Δm actually is important to clarify the validity of the present models.

4.2. Ellipticity of image deformation

Since d_A^l and d_A^t are different for the sources of $z > z_1^l$, their images are deformed and the degrees of deformation depend on ϕ . Here we define the ellipticity e by

$$\frac{1+e}{1-e} = \frac{d_A^l}{d_A^t} \quad \text{or} \quad e = \frac{d_A^l - d_A^t}{d_A^l + d_A^t}. \quad (32)$$

The z dependence of e was calculated in two model parameters for the study of its general behavior. The maximum and minimum of e are in $\phi \sim \pi/2$ and $\phi = 0, \pi$, respectively. To clarify the ϕ dependence of e , we derived the average value for $0 < \phi < \pi$, and the values averaged for $\phi < \pi/4, \pi/4 < \phi < 3\pi/4$, and $\phi > 3\pi/4$. Their results are shown in Figs. 10 and 11. It is found that the ellipticity e increases abruptly directly after the epoch $z = z_1^l$ and decreases gradually with z . Accordingly, we should measure the images of the sources around $z = z_1^l$ to confirm the lens effect.

5. Time-delay for a remote double quasar

The time-delay for a remote double source is basically caused by the geometrical length difference and gravitational redshift around the lens object, and so the formula in the present situation is the same as that in the homogeneous models. It is expressed (Sasaki 1993; Blandford and Narayan 1986; Schneider et al. 1992) as

$$\Delta t = \Delta t_{\text{geom}} + \Delta t_{\text{grav}}, \quad (33)$$

where

$$\Delta t_{\text{geom}} = \mathcal{D} C_{\text{geom}}, \quad \mathcal{D} \equiv \frac{D_l D_s}{D_{ls}}, \quad C_{\text{geom}} \equiv \frac{1}{2} (1 + z_l) (\boldsymbol{\theta} - \boldsymbol{\phi})^2, \quad (34)$$

$$\Delta t_{\text{grav}} = (D_l)^2 C_{\text{grav}}, \quad C_{\text{grav}} \equiv -\frac{1}{\pi} (1 + z_l) \int d\boldsymbol{\theta}'^2 \Sigma(\boldsymbol{\theta}') \ln[|\boldsymbol{\theta} - \boldsymbol{\theta}'|/\theta_c]. \quad (35)$$

Angular diameter distances D_l , D_s and D_{ls} denote the distances between an observer O and a lens L, between O and a source S, and between L and S, respectively. The angle vector $\boldsymbol{\theta}$ indicates the position of the ray relative to L in the lens plane, θ_c denotes the critical angle of the lens object, and $\Sigma(\boldsymbol{\theta})$ is the surface density. Another angle vector $\boldsymbol{\phi}$ indicates the position of S relative to L. For a double quasar we have the difference of time-delays $\delta \Delta t \equiv \mathcal{D} \delta C_{\text{geom}} + (D_l)^2 \delta C_{\text{grav}}$, where the differences of coefficients δC_{geom} and δC_{grav} are determined if the relative positions of L and S and the mass distribution in L are given.

If $z_s > z_1^l$, both L and S are in V^{II} , so that in the above formulas D_{ls} is given by $D_{ls} = D_A(\Omega_0^{II}, H_0^{II}, z_l, z_s)$, as in the homogeneous models, where

$$D_A(\Omega_0, H_0, z_l, z_s) \equiv \frac{2(c/H_0)}{\Omega_0^2 (1 + z_l) (1 + z_s)^2} \quad [(2 - \Omega_0 + \Omega_0 z_s) (1 + \Omega_0 z_l)^{1/2} \\ - (2 - \Omega_0 + \Omega_0 z_l) (1 + \Omega_0 z_s)^{1/2}]. \quad (36)$$

If we derive the effective Hubble constant $(H_0)_{\text{eff}}$ from the time-delay measurement, we have the relation $(H_0)_{\text{eff}} \propto 1/\delta\Delta t$. For a homogeneous model with Ω_0^{I} and H_0^{I} , moreover, we have the relation $H_0^{\text{I}} \propto 1/[\delta\Delta t]_{\text{homog}}$. From these two relations we obtain

$$\frac{H_0^{\text{I}}}{(H_0)_{\text{eff}}} = \frac{\delta\Delta t}{[\delta\Delta t]_{\text{homog}}} = \frac{\alpha_1 + \alpha_2\beta}{1 + \beta}, \quad (37)$$

where $\alpha_1 \equiv \mathcal{D}/\mathcal{D}_{\text{homog}}$, $\alpha_2 \equiv (D_l)^2/(D_l)_{\text{homog}}^2$, and $\beta \equiv [\mathcal{D}/(D_l)^2]_{\text{homog}}\delta C_{\text{geom}}/\delta C_{\text{grav}} (> 0)$. By solving this equation, therefore, we can obtain H_0^{II} in the present single-shell models. Since the lensing is caused in V^{II} , it is natural that we can get some informations about H_0^{II} and Ω_0^{II} from the time-delay measurement.

In the two single-shell models, by the way, we numerically obtain the following ratios (α_1 and α_2) of \mathcal{D} and $(D_l)^2$ to the corresponding ones in the homogeneous models with Ω_0^{I} and H_0^{I} , for the representative double quasar: 0957+561 ($z_l = 0.36$, $z_s = 0.41$).

For $(\Omega_0^{\text{I}}, \Omega_0^{\text{II}}, h^{\text{I}}, h^{\text{II}}/h^{\text{I}}) = (0.2, 0.56, 0.7, 0.82)$,

$$\alpha_1 = 1.01, \quad \alpha_2 = 1.16, \quad (38)$$

and $(\Omega_0^{\text{I}}, \Omega_0^{\text{II}}, h^{\text{I}}, h^{\text{II}}/h^{\text{I}}) = (0.2, 0.88, 0.7, 0.82)$,

$$\alpha_1 = 1.14, \quad \alpha_2 = 1.25. \quad (39)$$

If we take $(H_0)_{\text{eff}} \simeq 62 \text{ km s}^{-1} \text{ Mpc}^{-1}$ (Falco et al. 1997) and adopt $H_0^{\text{I}} = 70 \text{ km s}^{-1} \text{ Mpc}^{-1}$, the ratio (37) is $H_0^{\text{I}}/(H_0)_{\text{eff}} \simeq 1.13$, which is consistent with the above values (38) and (39) for $\beta \approx 1$.

6. Concluding remarks

In this paper we derived the angular diameter distances from central and non-central observers in the “cosmological void models”, for which we adopted the model parameters necessary to explain the bulk flow (derived in the previous paper (Tomita 1999)), and showed that the [m, z] relation due to these distances may explain the observed deviation of high-redshift supernovas (SNIa) from the relation in homogeneous Friedmann models, independently of the cosmological constant. This is possible because the void-like low-density region with a high Hubble parameter gives some “acceleration” to light coming from the high-density region with a low Hubble parameter, as if we were in a universe dominated by the positive cosmological constant.

It was found that the remarkable difference between the relation in the present models and the relation in the cosmological-constant-dominated model appears at epoch $z \simeq 1.0$ or at the earlier stage. The observation of SNIa around this epoch is, therefore, important to discriminate these two models observationally.

The unique property of the present models is that the [m, z] relation is anisotropic, in contrast to the relation in homogeneous Friedmann models, and that the systematic image deformation

appears for the sources with $z > z_1^j$ (~ 0.067). The observations about the anisotropy and lens effect will also be useful to determine which of the two models is better.

The derivation of distances in models with the intermediate self-similar region was not treated here, but their behavior is basically similar to that in the double-shell models, though their analysis is somewhat more complicated.

A. Distances in models with double shells

A.1. Distances from the center of the inner region

The line-elements in the regions V^I , V^{II} and V^{III} are given by Eq. (1) with $j = I$, II and III , respectively. When S is in V^I , V^{II} and V^{III} , the angular diameter distance d_A is given by Eq. (2), Eq. (3) and

$$d_A = a^{III}(\bar{\eta}_s^{III}) \sinh \bar{\chi}_s^{III}, \quad (A1)$$

respectively, where the negative curvature was assumed also in V^{III} . When S in V^I and V^{II} , d_A has the same expressions (for given \bar{z}_1^I and \bar{z}_s^{II}), as in the single-shell model. When S in V^{III} , we have for the coordinates of the second shell $(\bar{\eta}_2^j, \bar{\chi}_2^j)$ and those of S , $(\bar{\eta}_s^{III}, \bar{\chi}_s^{III})$:

$$\bar{\eta}_1^{II} - \bar{\eta}_2^{II} = \bar{\chi}_2^{II} - \bar{\chi}_1^{II}, \quad (A2)$$

$$\bar{\eta}_2^{III} - \bar{\eta}_s^{III} = \bar{\chi}_s^{III} - \bar{\chi}_2^{III}, \quad (A3)$$

where $\bar{\eta}_2^{II}$, $\bar{\eta}_s^{III}$ are related to \bar{z}_2^{II} , \bar{z}_s^{III} by

$$\frac{1 + \bar{z}_2^{II}}{1 + \bar{z}_1^{II}} = \frac{\cosh \bar{\eta}_1^{II} - 1}{\cosh \bar{\eta}_2^{II} - 1}, \quad (A4)$$

$$\frac{1 + \bar{z}_s^{III}}{1 + \bar{z}_2^{III}} = \frac{\cosh \bar{\eta}_2^{III} - 1}{\cosh \bar{\eta}_s^{III} - 1}. \quad (A5)$$

In the same way as $\bar{z}_1^I = \bar{z}_1^{II}$ in the previous subsection, we have the equality of the shell redshifts $\bar{z}_2^{II} = \bar{z}_2^{III}$. Moreover, coordinates $(\bar{\eta}_2^{III}, \bar{\chi}_2^{III})$ are connected with $(\bar{\eta}_2^{II}, \bar{\chi}_2^{II})$ by Eqs. (I.A14) and (I.A15). Accordingly, D_A is uniquely determined for given $\bar{z}_1^I (= \bar{z}_1^{II})$, $\bar{z}_2^{II} (= \bar{z}_2^{III})$ and \bar{z}_s^{III} .

Here we calculated the average values of d_A and d_L ($= (1 + z^j)^2$) defined by Eq. (31) and the z dependence of $5 \log d_L$ and Δm are shown in Figs. 4 and 6, respectively.

A.2. Distances from a non-central observer O in the inner region

When S in V^I and V^{II} , d_A^l, d_A^t and φ_s are the same as those in the single-shell model.

When S in V^{III} , we have

$$d_A^l \equiv d_A(\eta_s^{III}, \chi_s^{III}) \partial \varphi_s / \partial \phi / [\cos(\phi - \varphi_s)], \quad (A6)$$

$$d_A^t = d_A(\eta_s^{III}, \chi_s^{III}) \sin \varphi_s / \sin \phi, \quad (A7)$$

where

$$d_A(\eta_s^{III}, \chi_s^{III}) = a^{III}(\eta_s^{III}) \sinh(\chi_s^{III}). \quad (A8)$$

The relation between $(\eta_s^{III}, \chi_s^{III}, \varphi_s)$ and $(\eta_0^I, \chi_0^I, 0)$ are given as follows by specifying $\bar{z}_1^I, \bar{z}_2^I, z_s^{III}$ and ϕ . In the second shell we have

$$G(\chi_2^{II}) \equiv \cosh^{-1} \left(\frac{\cosh \chi_2^{II}}{h_0^{II}} \right) - \cosh^{-1} \left(\frac{\cosh \chi_1^{II}}{h_0^{II}} \right) = \eta_1^{II} - \eta_2^{II}, \quad (A9)$$

and in V^{III}

$$G(\chi_s^{III}) \equiv \cosh^{-1} \left(\frac{\cosh \chi_s^{III}}{h_0^{III}} \right) - \cosh^{-1} \left(\frac{\cosh \chi_2^{III}}{h_0^{III}} \right) = \eta_2^{III} - \eta_s^{III}, \quad (A10)$$

where

$$h_0^{III} = [1 + (\zeta^{III})^2]^{1/2}, \quad \zeta^{III} = \frac{a_0^I}{a_0^{III}} \zeta^I. \quad (A11)$$

The coordinates $(\eta_2^{III}, \chi_2^{III})$ are related to $(\eta_2^{II}, \chi_2^{II})$, using

$$a_0^{II} y^{II}(\eta_2^{II}) \sinh \chi_2^{II} = a_0^{III} y^{III}(\eta_2^{III}) \sinh \chi_2^{III} \quad (A12)$$

and

$$a_0^{II} \int_0^{\eta_2^{II}} y^{II}(\eta) d\eta = a_0^{III} \int_0^{\eta_2^{III}} y^{III}(\eta) d\eta. \quad (A13)$$

Moreover, φ_2 is derived in V^{II} as

$$\begin{aligned} \varphi_2 = \varphi_1 &+ \tan^{-1} \left\{ \frac{1}{\zeta^{II}} \left[\sinh^2 \chi_2^{II} + \cosh \chi_2^{II} \sqrt{\sinh^2 \chi_2^{II} - (\zeta^{II})^2} \right] \right\} \\ &- \tan^{-1} \left\{ \frac{1}{\zeta^{II}} \left[\sinh^2 \chi_1^{II} + \cosh \chi_1^{II} \sqrt{\sinh^2 \chi_1^{II} - (\zeta^{II})^2} \right] \right\} \end{aligned} \quad (A14)$$

and in V^{III} we have

$$\begin{aligned} \varphi = \varphi_2 &+ \tan^{-1} \left\{ \frac{1}{\zeta^{III}} \left[\sinh^2 \chi^{III} + \cosh \chi^{III} \sqrt{\sinh^2 \chi^{III} - (\zeta^{III})^2} \right] \right\} \\ &- \tan^{-1} \left\{ \frac{1}{\zeta^{III}} \left[\sinh^2 \chi_2^{III} + \cosh \chi_2^{III} \sqrt{\sinh^2 \chi_2^{III} - (\zeta^{III})^2} \right] \right\}, \end{aligned} \quad (A15)$$

$$\varphi_s = \varphi(\chi^{III} = \chi_s^{III}). \quad (A16)$$

Thus φ_s was derived as a function of $\bar{z}_1^I, \bar{z}_2^I, z_s^{III}$ and ϕ ($= \phi_1$ or $\pi - \phi_1$).

The author thanks a referee for kind comments about past related works. This work was supported by Grant-in Aid for Scientific Research (No. 10640266) from the Ministry of Education, Science, Sports and Culture, Japan.

REFERENCES

Bartlett, J. G., Blanchard, A., Silk, J., and Turner, M. S. 1995, *Science*, 267, 980

Blandford, R. D. & Kundić, T. 1997, *The Extragalactic Distance Scale*, M. Livio, M. Donahue and N. Panagia, London: Cambridge University Press, 60

Blandford, R. and Narayan, R. 1986, *ApJ*, 310, 568

Branch, D. 1998, *ARA&A*, 36, 17

Dale, D. A., Giovanelli, R., and Haynes, M.P. 1999, *ApJ*, 510, L11

Falco, E. E. et al. 1997, *ApJ*, 484, 70

Freedman, W. L. 1997, *Critical Dialogues in Cosmology*, N. Turok, Singapore: World Scientific, 92

Garnavich, P. M. et al., 1998, *ApJ*, 493, L53

Giovanelli, R., Haynes, M. P., Freudling, W., da Costa, L. N., Salzer, J. J., and Wegner, G. 1998, *ApJ*, 505, L91

Hudson, M. J., Smith, R. J., Lucey, J. R., Schlegel D. J. and Davies, R. L. *ApJ*, L79 ; Hudson, M. J., Lucey, J. R., Smith, R. J., and Steel, J. 1997, *MNRAS*, 291, 488

Riess, A. G. et al. 1998, *AJ*, 116, 1009

Sandage, A. and Tammann, G.A. 1997, *Critical Dialogues in Cosmology*, N. Turok, Singapore: World Scientific, 130

Sasaki, M. 1993, *Prog. Theor. Phys.*, 90, 753

Schmidt, B. P. et al. 1998, *ApJ*, 507, 46

Schneider, P., Ehlers, J. and Falco, E. E. 1992, *Gravitational Lenses*, Berlin: Springer-Verlag

Tomita, K. 1999, *ApJ* in press, [astro-ph/9905278](#)

Tomita, K. 1996, *ApJ*, 461, 507

Tomita, K. 1995, *ApJ*, 451, 541; Tomita, K. 1996, *ApJ*, 464, 1054 for Erratum

Turner, E. L., Cen, R., and Ostriker, J. P. 1992, *AJ*, 103, 1427

Willick, J. A. 1999, *ApJ*, 516, 47; [astro-ph/9812470](#)

Zehavi, I., Riess, A. G., Kirshner, P. and Dekel, A. 1998, *ApJ*, 503, 483

Fig. 1.— A model with a single shell. z and \bar{z} are the redshifts for observers at O and C.

Fig. 2.— The relation between d_A and z . A solid line (a) and a short dash line (b) represent the single-shell model with $(\Omega_0^I, \Omega_0^{II}, h^I, h^{II}/h^I) = (0.2, 0.56, 0.7, 0.82)$. (a) denotes the ϕ averaged value by the observer O and (b) denotes the case of the virtual observer C. (c) and (d) stand for the homogeneous models with $(\Omega_0, \lambda_0) = (0.2, 0)$ and $(0.2, 0.8)$, respectively.

Fig. 3.— The relation between d_A and z . A solid line (a) and a short dash line (b) represent the single-shell model with $(\Omega_0^I, \Omega_0^{II}, h^I, h^{II}/h^I) = (0.2, 0.88, 0.7, 0.82)$. The other meaning of lines is the same as that in Fig. 2.

Fig. 4.— The relation between d_A and z . A long dash line (a) and a short dash line (b) represent the double-shell models with $(\Omega_0^I, \Omega_0^{II}, \Omega_0^{III}, h^I, h^{II}/h^I, h^{III}/h^I) = (0.2, 0.56, 0.88, 0.7, 0.92, 0.82)$, $(0.2, 0.36, 0.56, 0.7, 0.92, 0.82)$, respectively, for the observer C. (c) denotes the line by the observer C in the single-shell model with $(\Omega_0^I, \Omega_0^{II}, h^I, h^{II}/h^I) = (0.2, 0.56, 0.7, 0.82)$. (d) denotes the Friedmann model with $\Omega_0 = 0.2$.

Fig. 5.— The z dependence (in the single-shell models) of the magnitude difference Δm relative to the magnitude in the Friedmann model with the same Ω_0 . Lines (a), (b), (c) and (d) stand for the parameters $(\Omega_0^I, \Omega_0^{II}, h^I, h^{II}/h^I) = (0.2, 0.56, 0.7, 0.82)$, $(0.2, 0.88, 0.7, 0.82)$, $(0.3, 0.56, 0.7, 0.82)$, $(0.3, 0.88, 0.7, 0.82)$, respectively, for $z_1 = 0.067$. (e) denote the case $(0.2, 0.56, 0.7, 0.82)$ for $z_1 = 0.1$. (f) denotes the homogeneous model with $(\Omega_0, \lambda_0) = (0.2, 0.8)$.

Fig. 6.— The z dependence (in the double-shell models) of the magnitude difference Δm relative to the magnitude in the Friedmann model with the same Ω_0 . Lines (a) and (b) stand for $(\Omega_0^I, \Omega_0^{II}, \Omega_0^{III}, h^I, h^{II}/h^I, h^{III}/h^I) = (0.2, 0.36, 0.56, 0.7, 0.92, 0.82)$, $(0.2, 0.56, 0.88, 0.7, 0.92, 0.82)$, respectively, with $z_1 = 0.05$ and $z_2 = 0.1$. (c) is shown for comparison in the single-shell model with $(\Omega_0^I, \Omega_0^{II}, h^I, h^{II}/h^I) = (0.2, 0.56, 0.7, 0.82)$ and $z_1 = 0.067$.

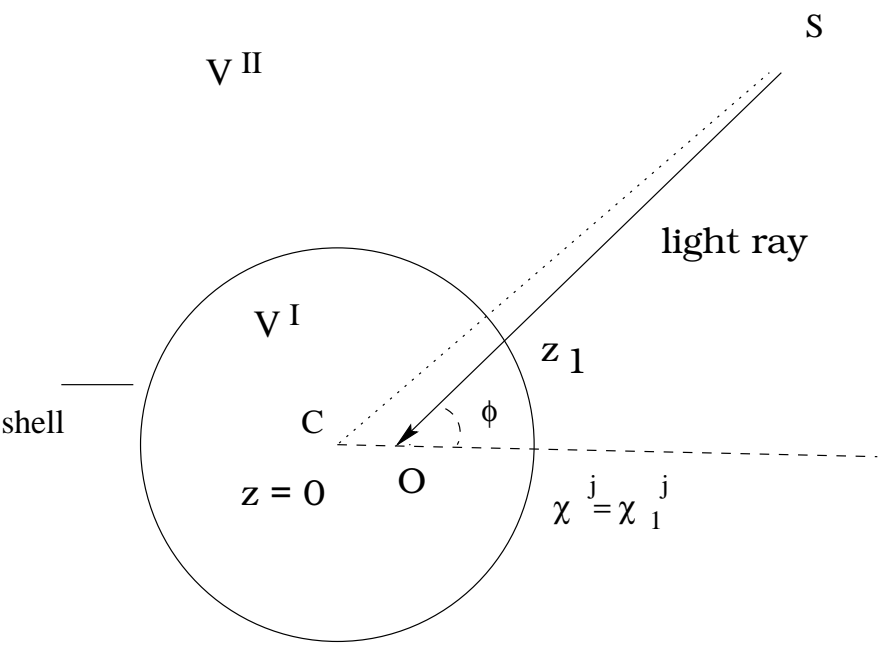
Fig. 7.— Planes with constant θ .

Fig. 8.— The z dependence of the magnitude difference Δm relative to the magnitude in the Friedmann model with the same Ω_0 for the observer O in the single-shell model with $(\Omega_0^I, \Omega_0^{II}, h^I, h^{II}/h^I) = (0.2, 0.56, 0.7, 0.82)$. Lines (a), (b) and (c) stand for the values averaged for $\phi < \pi/4, \pi/4 < \phi < 3\pi/4$, and $\phi > 3\pi/4$, respectively. For comparison (d) stands for the value by the observer C and (e) is for the homogeneous model with $(\Omega_0, \lambda_0) = (0.2, 0.8)$.

Fig. 9.— The z dependence of the magnitude difference Δm relative to the magnitude in the Friedmann model with the same Ω_0 for the observer O in the single-shell model with $(\Omega_0^I, \Omega_0^{II}, h^I, h^{II}/h^I) = (0.2, 0.88, 0.7, 0.82)$. The meaning of suffices are the same as those in Fig. 8.

Fig. 10.— The z dependence of the ellipticity e for the observer O in the single-shell model with $(\Omega_0^I, \Omega_0^{II}, h^I, h^{II}/h^I) = (0.2, 0.56, 0.7, 0.82)$. Lines (b), (c) and (d) stand for the values averaged for $\phi < \pi/4, \pi/4 < \phi < 3\pi/4$, and $\phi > 3\pi/4$, respectively. (a) denotes the value averaged for $0 < \phi < \pi$.

Fig. 11.— The z dependence of the ellipticity e for the observer O in the single-shell model with $(\Omega_0^I, \Omega_0^{II}, h^I, h^{II}/h^I) = (0.2, 0.88, 0.7, 0.82)$. the suffices are the same as those in Fig. 10.



$$\bar{z}_1 = 0.067$$

